Journal of Advanced Ceramics
2013, 2(4): 318–324
DOI: 10.1007/s40145-013-0078-5

ISSN 2226-4108
CN 10-1154/TQ

Research Article

Processing and characterization of polymer precursor derived silicon oxycarbide ceramic foams and compacts

Srinivasan NEDUNCHEZHIAN, Ravindran SUJITH, Ravi KUMAR*

Materials Processing Section, *Department of Metallurgical and Materials Engineering*, *Indian Institute of Technology Madras*, *Chennai 600036*, *Tamil Nadu*, *India*

Received: May 27, 2013; Revised: July 22, 2013; Accepted: August 08, 2013

Abstract: This work focused on the fabrication of silicon oxycarbide ceramic (SiOC) foams as well as dense compacts using poly(hydridomethylsiloxane) (PHMS) as a polymer precursor. The room-temperature cross-linking of PHMS was achieved by the addition of 1,4-diazabicyclo [2.2.2] octane (DABCO) with the release of hydrogen gas as a by-product. This resulted in self-blowing of the polymer precursor at room temperature and thereby offered the possibility of producing SiOC foams without the need of any external blowing agents. We also reported the fabrication of crack-free silicon oxycarbide compacts by cold compaction and pyrolysis route using polyvinyl alcohol (PVA) as a processing additive. Cylindrical-shaped pellets were pyrolysed at 1300 ℃ in argon atmosphere with a ceramic yield of approximately 85%. Increased resistance to phase separation and crystallization up to 1400 ℃ was attributed to the presence of large volume fraction of free carbon in the material which was confirmed by Raman spectroscopy.

Keywords: silicon oxycarbide; foams; 1,4-diazabicyclo [2.2.2] octane (DABCO); self-blown polymer; poly(hydridomethylsiloxane) (PHMS)

1 Introduction

Silicon oxycarbide ceramic (SiOC) processed through polymer precursors is one of the widely studied systems due to its attractive thermo-mechanical properties [1–6]. This is attributed to the replacement of a part of its divalent oxygen atoms by the tetravalent carbon atoms, resulting in a stronger 3-dimensional network in contrast to silica, thereby enhancing the potential of the material [7]. Polysiloxanes are widely-used polymer precursors for the production of SiOC because of the ease of availability, low cost and flexibility to handle in atmospheric ambience. Wide varieties of polysiloxanes are available in the market including poly(hydroxymethylsiloxane), poly (methylsilsesquioxane), poly(methylphenylsiloxane) and poly(hydridomethylsiloxane) (PHMS) to produce SiOC upon pyrolysis. However, the final chemical composition, ceramic yield, carbon content and thermal stability depend on the side-chain constituent (hydrogen, methyl or phenyl groups) of the polymer precursor [8]. The current study focuses on the processing of SiOC from PHMS since it contains functional hydrogen group in its side-chain which is

* Corresponding author.
E-mail: nvrk@iitm.ac.in

beneficial for cross-linking.

SiOC derived from PHMS requires necessarily a cross-linking step since linear polymers undergo complete thermal decomposition during pyrolysis treatment. Earlier investigation focused primarily on cross-linking of PHMS through the hydrosilylation reaction by mixing with vinyl containing precursor catalyzed by platinum-based complexes resulting in higher ceramic yield upon pyrolysis [9–12]. However, cross-linking through hydrosilylation reaction requires additional vinyl group containing precursor and platinum-based catalysts which are expensive. Here, we report rather a simple method of cross-linking PHMS at room temperature by the addition of inexpensive 1,4-diazabicyclo [2.2.2] octane (DABCO) catalyst and the ceramic yield obtained was comparable to the one achieved through cross-linking by hydrosilylation reaction. However, generation of gaseous by-product during cross-linking resulted in self-blowing, thereby producing ceramic foams. This reaction was explored to produce ceramic foams.

For the production of bulk compacts, cold compaction technique was adopted by applying a uniaxial load on cross-linked precursor powder. Fabrication of bulk compacts through polymer derived ceramic route is always a challenge because of its associated porosity and volumetric shrinkage during polymer to ceramic conversion [13]. This necessitates the use of active and passive fillers to counteract very high volumertric shrinkage during pyrolysis [14]. Here, in this paper we report an economical way of processing filler-free bulk SiOC through cold compaction using polyvinyl alcohol (PVA) as a processing additive.

2 Experiment

Commercially available PHMS ($(CH_3)_3$–Si(O)–$[CH_3(H)Si–O]_n$–$Si(CH_3)_3$) (Sigma Aldrich, India) was used as the starting polymeric precursor. The room-temperature cross-linking of precursor was achieved by the addition of 5 wt% DABCO (Sigma Aldrich, India). The solution was thoroughly mixed in a teflon beaker which was subsequently kept overnight for cross-linking. Teflon beaker was used in all the experiments to enable easy removal of the cross-linked polymer. The amount of DABCO catalyst added had a profound influence on the gelation time of the precursor (liquid to solid). The addition of 2 wt% DABCO catalyst took almost 24 h for complete cross-linking. In order to reduce the gelation time, ~5 wt% DABCO catalyst was used for cross-linking PHMS. Subsequently, foamed polymer was subjected to pyrolysis treatment in an alumina tubular furnace by heating to 1000 ℃ in a flowing argon gas atmosphere (purity 99.9%, flow rate 5 L/min) at a heating rate of 5 ℃/min for 2 h and the furnace cooled to produce SiOC foams.

For producing dense SiOC, cross-linked polymer was ground to fine powder using agate pestle and mortar. To improve the green strength of the pellets, 2 drops of 4% PVA solution was added to 0.75 g of polymer precursor powder prior to cold compaction. Cold uniaxial pressing was carried out in a compaction unit (Insmart XRF 40, India, capacity 40 tonnes) using zinc stearate as a lubricant by applying a compaction pressure of 440 MPa for 1 min in a cylindrical die made of cold rolled steel. It was observed that compaction carried out at a pressure greater than 440 MPa resulted in cracking of the samples during pyrolysis. Hence, all the green compacts were produced limiting the pressure to 440 MPa. Cylindrical-shaped green pellets with diameter of 12 mm and thickness of 7 mm were produced after compaction. Subsequently, cold compacted samples were pyrolyzed at 1300 ℃ for 2 h in argon to produce dense SiOC compacts. The elemental composition of as-thermolysed SiOC was assumed to be identical to the composition reported by Blum *et al.* [15].

Thermogravimetric (TG) analysis (NETZSCH STA 409 PC/PG, Germany) was performed by heating 5 mg of samples taken in an alumina crucible from room temperature to 1000 ℃ at a heating rate of 5 ℃/min in a flowing argon atmosphere (flow rate 50 ml/min). Fourier-transformed infrared (FT-IR) spectrometer (Perkin Elmer Spectrum One, USA) was used to record transmittance spectra of samples in the range of 4000–400 cm^{-1} with a resolution of 4 cm^{-1}. X-ray diffraction (XRD) analysis was carried out on samples pyrolyzed in argon at temperatures ranging from 1000 ℃ to 1400 ℃ using D8 Discover, Bruker AXS X-ray diffractometer (USA) with Cu Kα radiation. The voltage and current settings used were 35 kV and 25 mA, respectively. All pyrolyzed ceramic samples were scanned from 5° to 90° (2θ) at a scan speed of 1 s/step. The foam morphology and presence of porosity were investigated using FEI scanning electron microscopy (SEM, Quanta 200, USA). The Raman

spectra of pyrolyzed ceramic were obtained with the help of confocal Raman spectrometer (WITEC alpha 300, Germany) using Nd:YAG laser (wavelength 532 nm). The density of bulk ceramic samples produced by cold compaction and pyrolysis route were measured using both Archimedes' principle and geometrical method. The density of foam samples were calculated by measuring the weight and the volume.

3 Results and discussion

3.1 Characterization of polymer precursor

The FT-IR spectra of the as-received polymer and cross-linked polymer are exemplified in Fig. 1. The broad intense peak centred at 1100 cm^{-1} is attributed to Si–O–Si asymmetric vibration which is typical of any siloxane. The peaks observed at 1400 cm^{-1} and 1200 cm^{-1} in the as-received PHMS are attributed to Si–CH_3 asymmetric and symmetric bending vibrations, respectively. Moreover, the C–H stretching vibration is observed at 2966 cm^{-1} and 2901 cm^{-1}. The sharp intense peaks at 2166 cm^{-1} and 755 cm^{-1} are assigned to Si–H stretching and Si–C stretching, respectively. However, in contrast to the FT-IR spectra of the as-received PHMS, sharp decreases in the intensity of the peaks at 2166 cm^{-1} and 2966 cm^{-1} are observed in the cross-linked PHMS attributing to the dehydrocoupling reaction. Accordingly, the most probable cross-linking mechanism is explained in Scheme 1, which is in accordance with the earlier reports [16–18]. This reaction occurs at room temperature catalyzed by the addition of DABCO catalyst. Neverthelesss, it is noteworthy that even after cross-linking, Si–H peak is observed in the FT-IR spectrum of the cross-linked PHMS indicating that hydrogen is not completely consumed during cross-linking. Since the initial polymer contains reactive group (hydrogen) in its side-chain, it helps in cross-linking at room temperature by the addition of DABCO catalyst. Similar types of dehydrocoupling reactions were also reported in polysilazanes with reactive groups such as Si–H and N–H by the addition of appropriate catalyst [19]. And, also yield upon thermolysis is significantly improved because of higher dimensional cross-linked polymer molecular structure [20]. The cross-linking yield is approximately 99% and the 1% mass loss observed during cross-linking could be due to the loss of lower molecular weight groups in the polymer which is hydrogen in this case (Scheme 1).

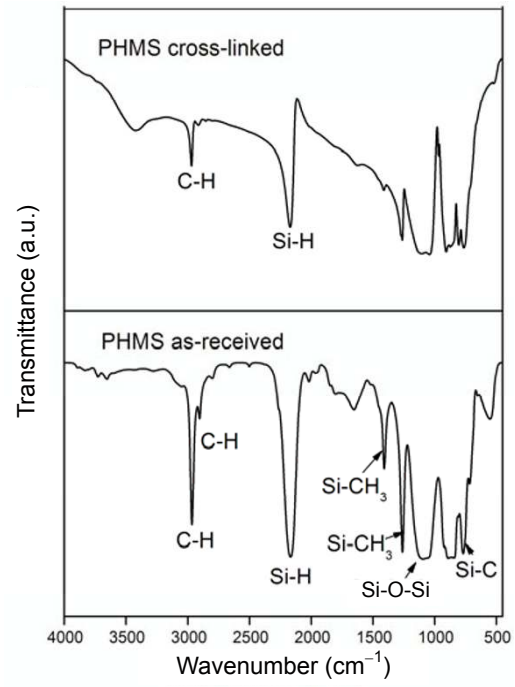

Fig. 1 FT-IR spectra of the as-received polymer and cross-linked polymer.

Scheme 1 Cross-linking mechansim deduced from FT-IR spectra is:

$$Si–H + H–Si \rightarrow Si–Si + H_2$$

$$C–H + H–Si \rightarrow Si–Si + H_2$$

TG analysis of the cross-linked polymer in argon atmosphere shows that organic to inorganic transition starts at around 100 ℃ with loss of residual hydrogen and ends at ~900 ℃, resulting in SiOC with ~85% yield (Fig. 2(b)). This matches with the experimentally measured yield by taking the ratio of the weight of the

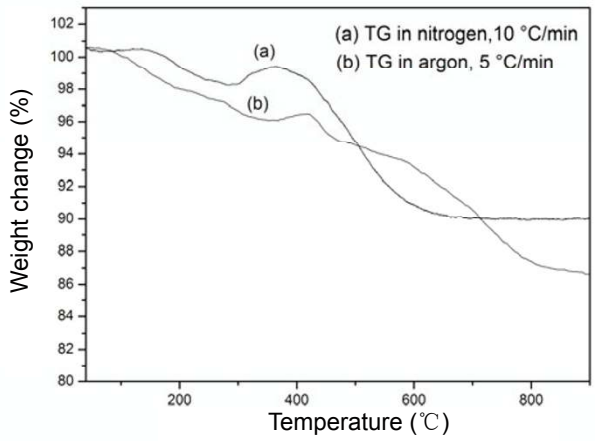

Fig. 2 TG analysis of cross-linked polymer in (a) nitrogen and (b) argon atmosphere.

ceramic obtained to the weight of the polymer taken. A small weight gain in the temperature range of around 390–410 ℃ is also observed. TG analysis in nitrogen atmosphere (Fig. 2(a)) at a heating rate of 10 ℃/min also shows a similar weight gain of ~1% but at a different temperature range of 320–400 ℃ which could be due to the difference in heating rate and change in atmosphere. Moreover, from the TG data it could be inferred that the ceramic yield is higher in nitrogen atmosphere (~88%) in comparison to argon atmosphere, implying the significance of processing atmosphere.

3.2 XRD and spectroscopic characterization of SiOC

The XRD of the SiOC samples pyrolysed between 1000 ℃ and 1400 ℃ are shown in Fig. 3. Complete absence of phase separation and crystallization up to 1300 ℃ and only a broad amorphous hump at $2\theta = 21°$ corresponding to the most intense peak of silicon dioxide (cristobalite) are observed. However, samples exposed to 1400 ℃ for longer duration (10 h) result in the phase separation of silicon dioxide and β-silicon carbide from the amorphous SiOC network (Fig. 3).

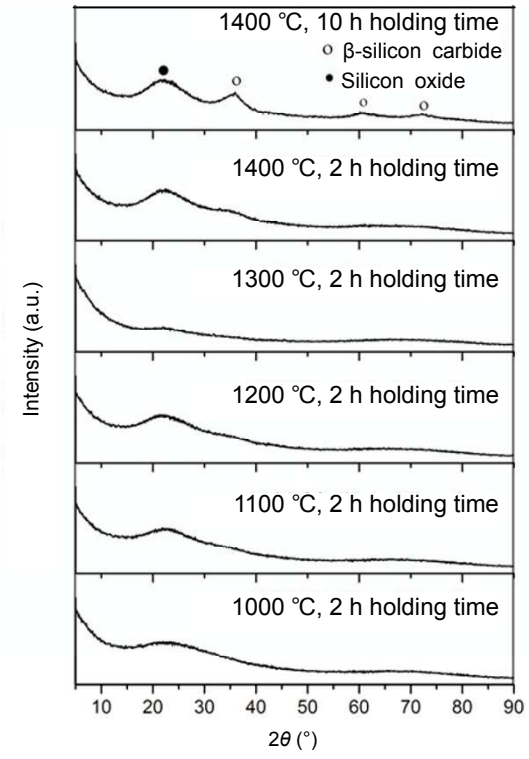

Fig. 3 X-ray diffractograms of the as-thermolysed and heat-treated SiOC samples.

Silicon carbide peaks ($2\theta = 35.5°$, 61° and 72°) start to appear for the samples pyrolysed at 1400 ℃ for 10 h. However, the peaks are broad indicating the nanocrytalline nature of SiC. The crystallite size of β-SiC measured by Scherrer method is ~2.5 nm inferring the insignificant crystallite coarsening. This could be in accodance with the method suggested by Walter *et al*. [21], in which the presence of free carbon was reported to restrict the mobility of SiC in the SiOC network. However, the presence of graphite-like carbon/free carbon is not revealed in the X-ray diffractograms. Nevertheless, Raman spectrum of SiOC sample heat treated at 1400 ℃ shows characteristic peaks (D and G bands) of free carbon phase (Fig. 4). D band observed at 1344 cm^{-1} corresponds to disorderness in the sp^2 carbon (breaking of translational symmetry) and G band observed at 1605 cm^{-1} corresponds to tangential vibration mode of graphite [22]. In addition, the limited crystallite growth of β-SiC could also be attributed to the high viscosity of SiOC (~10^{14}–10^{16} Pa·s) as proposed by Schiavon *et al*. [23] and Rouxel *et al*. [24].

3.3 Ceramic foams

The hydrogen evolution during cross-linking results in self-blowing of the polymer as explained schematically in Fig. 5. Bubbles of hydrogen nucleate at the bottom of the container and move upwards resulting in the formation of localized colonies followed by the growth of existing bubbles at the expense of newly formed bubbles. The continous bubble formation followed by stabilization results in blowing of the entire polymer. Elongated pores oriented along the foaming direction are observed in a foamed precursor. The foam structure is retained during the pyrolysis treatment. The

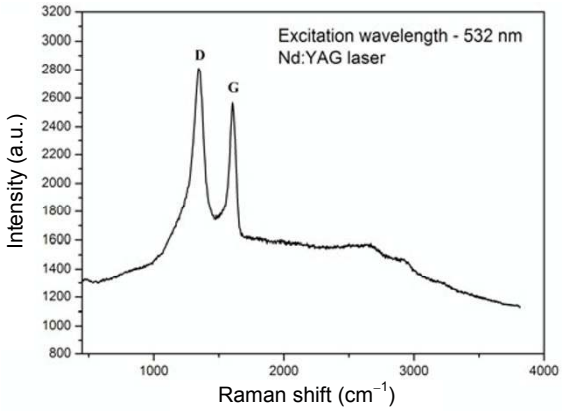

Fig. 4 Raman spectrum of the sample heat treated at 1400 ℃ for 10 h.

self-blowing of poly(phenylmethylsilsesquioxane) at 300 ℃ due to release of water and ethanol was reported in the literatures by Gambaryan-Roisman *et al*. [25] and Zeschky *et al*. [26–28]. This method of producing SiOC foams is promising, since the removal of sacrificial phase during pyrolysis is not required. However, it is often difficult to control the density of ceramic foams processed through this method. The photographs and SEM images of pyrolyzed ceramic foams is shown in Figs. 6(a) and 6(b) indicating that the processed foams are relatively free of cracks.

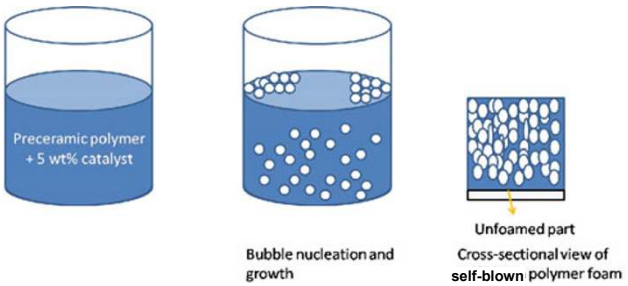

Fig. 5 Schematic chart of self-blowing phenomenon in PHMS.

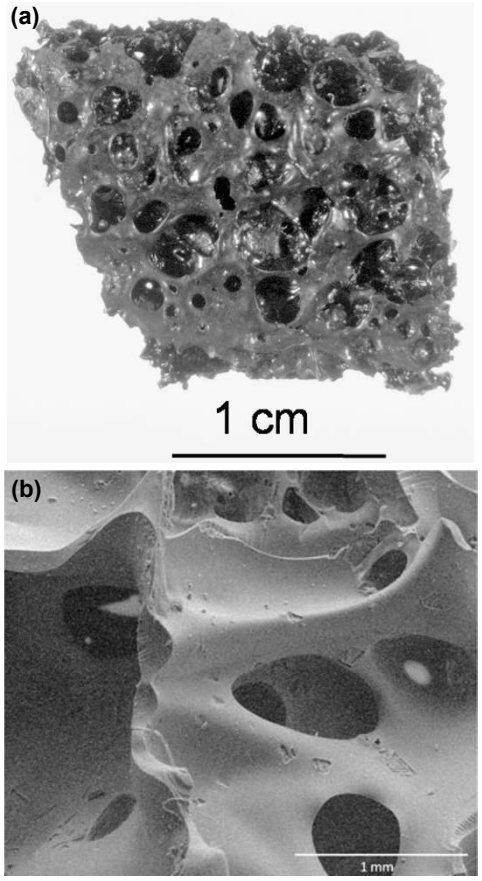

Fig. 6 (a) Photograph of SiOC foams; (b) SEM showing interconnected porosity in SiOC foams.

3.4 Bulk compacts

The photographs of the cold compacted pellet and the SiOC compact after pyrolysis are shown in Fig. 7. An optimized compaction pressure of 440 MPa was used for the processing of bulk compacts, since residual porosity in the green stage for gaseous by-products to escape during pyrolysis is always desired. It is observed that the addition of PVA reduces the free flowability of powder thereby retaining the shape after pressing. However, in contrast to warm pressing where welding and plastic deformation occur at the pressing temperature, only particle rearrangement occurs in cold pressing and PVA plays a vital role in producing bulk compacts. This is supported by the SEM images of cross-linked polymer powder particles and pyrolyzed SiOC as shown in Figs. 8(a) and 8(b), respectively. Individual particles could be seen even after the pyrolysis with residual irregular shaped pores (Fig. 8(b)). The density of pyrolyzed samples is 1.4–1.5 g/cm^3 and geometric density is close to 1.5–1.6 g/cm^3. Compared to the density values reported in the existing literatures for SiOC [29–31], the observed density is lower for the cold pressed and pyrolysed SiOC. This could be attributed to the presence of residual porosity due to the escapement of volatile matter during the thermolysis. However, the linear shrinkages in axial and radial directions are ~26% and ~27% respectively and the volumetric shrinkage is ~67%. Harshe *et al*. [7] and Weisbarth and Jansen [32] reported axial shrinkage of ~16% and ~19% for bulk SiOC and $SiBN_3C$, respectively. Henceforth, the shrinkage occuring in these ceramics could be considered as a useful indication of densification. Despite the fact that very high linear shrinkage is observed, crack-free SiOC is obtained after pyrolysis and is mainly attributed to isotropic shrinkage and high ceramic yield of polymer precursor.

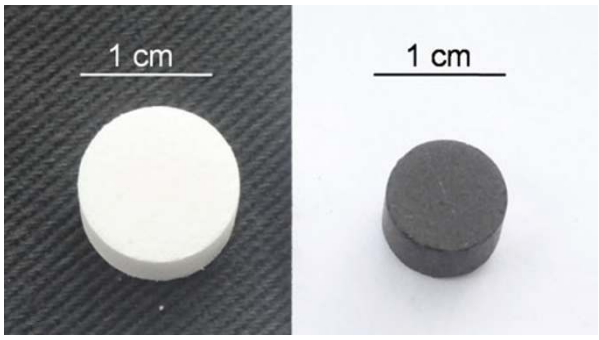

Fig. 7 Photographs of cold compacted SiOC samples before and after pyrolysis.

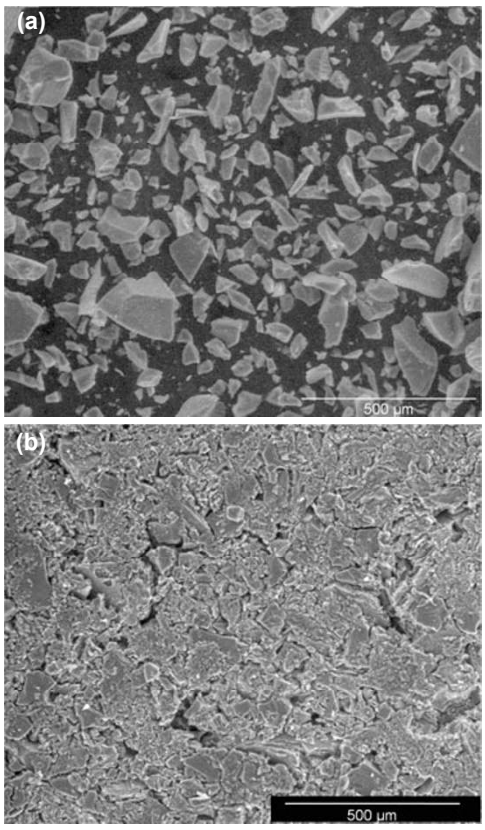

Fig. 8 SEM images of cross-linked polymer powder and pyrolyzed ceramic.

4 Conclusions

Room-temperature cross-linking of PHMS was achieved by the addition of DABCO catalyst with a ceramic yield of approximately 85%. SiOC was thermally stable (absence of phase separation) up to 1300 ℃ in argon atmosphere. Crystalline peaks corresponding to β-SiC were observed only after prolonged exposure at 1400 ℃. The presence of free carbon was confirmed by Raman spectroscopy. SEM micrographs revealed the presence of porosity in optimized SiOC compacts and interconnected pores in self-blown ceramic foams. Filler-free monolithic SiOC compacts using PVA as a binder were found to be promising and economical. SiOC foams through self-blowing mechanism were found to be attractive because of the ease in processability in contrast to other processing routes.

Acknowledgements

This work was supported financially by Indian Space Research Organisation and their support is gratefully acknowledged.

References

[1] Zhang H, Pantano CG. Synthesis and characterization of silicon oxycarbide glasses. *J Am Ceram Soc* 1990, **73**: 958–963.

[2] Renlund GM, Prochazka S, Doremus RH. Silicon oxycarbide glasses: Part II. Structure and properties. *J Mater Res* 1991, **6**: 2723–2734.

[3] Bois L, Maquet J, Babonneau F, *et al*. Structural characterization of sol–gel derived oxycarbide glasses. 1. Study of the pyrolysis process. *Chem Mater* 1994, **6**: 796–802.

[4] Corriu RJP, Leclercq D, Mutin PH, *et al*. ^{29}Si nuclear magnetic resonance study of the structure of silicon oxycarbide glasses derived from organosilicon precursors. *J Mater Sci* 1995, **30**: 2313–2318.

[5] Mutin PH. Control of the composition and structure of silicon oxycarbide and oxynitride glasses derived from polysiloxane precursors. *J Sol–Gel Sci Technol* 1999, **14**: 27–38.

[6] Kleebe HJ, Turquat C, Sorarù GD. Phase separation in an SiCO glass studied by transmission electron microscopy and electron energy-loss spectroscopy. *J Am Ceram Soc* 2001, **84**: 1073–1080.

[7] Harshe R, Balan C, Riedel R. Amorphous Si(Al)OC ceramic from polysiloxanes: Bulk ceramic processing, crystallization and applications. *J Eur Ceram Soc* 2004, **24**: 3471–3482.

[8] Colombo P, Mera G, Riedel R, *et al*. Polymer-derived ceramics: 40 years of research and innovation in advanced ceramics. *J Am Ceram Soc* 2010, **93**: 1805–1837.

[9] Radovanovic E, Gozzi MF, Gonçalves MC, *et al*. Silicon oxycarbide glasses from silicone networks. *J Non-Cryst Solids* 1999, **248**: 37–48.

[10] Modena S, Sorarù GD, Blum Y, *et al*. Passive oxidation of an effluent system: The case of polymer-derived SiCO. *J Am Ceram Soc* 2005, **88**: 339–345.

[11] Liu X, Li YL, Hou F. Fabrication of SiOC ceramic microparts and patterned structures from polysiloxanes via liquid cast and pyrolysis. *J Am*

Ceram Soc 2009, **92**: 49–53.

[12] Su D, Li YL, An HJ, *et al*. Pyrolytic transformation of liquid precursors to shaped bulk ceramics. *J Eur Ceram Soc* 2010, **30**: 1503–1511.

[13] Jiang T, Hill A, Fei W, *et al*. Making bulk ceramics from polymeric precursors. *J Am Ceram Soc* 2010, **93**: 3017–3019.

[14] Greil P. Active-filler-controlled pyrolysis of preceramic polymers. *J Am Ceram Soc* 1995, **78**: 835–848.

[15] Blum YD, MacQueen DB, Kleebe H-J. Synthesis and characterization of carbon-enriched silicon oxycarbides. *J Eur Ceram Soc* 2005, **25**: 143–149.

[16] Lavedrine A, Bahloul D, Goursat P, *et al*. Pyrolysis of polyvinylsilazane precursors to silicon carbonitride. *J Eur Ceram Soc* 1991, **8**: 221–227.

[17] Yvie NSCK, Corriu RJP, Leclerq D, *et al*. Silicon carbonitride from polymeric precursors: Thermal cross-linking and pyrolysis of oligosilazane model compounds. *Chem Mater* 1992, **4**: 141–146.

[18] Wen G, Bai H, Huang X, *et al*. Lotus-type porous SiOCN ceramic fabricated by undirectional solidification and pyrolysis. *J Am Ceram Soc* 2011, **94**: 1309–1313.

[19] Kroke E, Li Y-L, Konetschny C, *et al*. Silazane derived ceramics and related materials. *Mat Sci Eng R* 2000, **26**: 97–199.

[20] Blum YD, Schwartz KB, Laine RM. Preceramic polymer pyrolysis. *J Mater Sci* 1989, **24**: 1707–1718.

[21] Walter S, Soraru GD, Bréquel H, *et al*. Microstructural and mechanical characterization of sol–gel-derived Si–O–C glasses. *J Eur Ceram Soc* 2002, **22**: 2389–2400.

[22] Wang Y, Alsmeyer DC, McCreery RL. Raman spectroscopy of carbon materials: Structural basis of observed spectra. *Chem Mater* 1990, **2**: 557–563.

[23] Schiavon MA, Gervais C, Babonneau F, *et al*. Crystallization behavior of novel silicon boron oxycarbide glasses. *J Am Ceram Soc* 2004, **87**: 203–208.

[24] Rouxel T, Soraru G-D, Vicens J. Creep viscosity and stress relaxation of gel-derived silicon oxycarbide glasses. *J Am Ceram Soc* 2001, **84**: 1052–1058.

[25] Gambaryan-Roisman T, Scheffler M, Buhler P, *et al*. Processing of ceramic foam by pyrolysis of filler containing phenylmethyl polysiloxane precursor. *Ceram Trans* 2000, **108**: 121–130.

[26] Zeschky J, Goetz-Neunhoeffer F, Neubauer J, *et al*. Preceramic polymer derived cellular ceramics. *Compos Sci Technol* 2003, **63**: 2361–2370.

[27] Zeschky J, Höfner T, Arnold C, *et al*. Polysilsesquioxane derived ceramic foams with gradient porosity. *Acta Mater* 2005, **53**: 927–937.

[28] Zeschky J, Lo J, Höfner T, *et al*. Mg alloy infiltrated Si–O–C ceramic foams. *Mat Sci Eng A* 2005, **403**: 215–221.

[29] Mazo MA, Palencia C, Nistal A, *et al*. Dense bulk silicon oxycarbide glasses obtained by spark plasma sintering. *J Eur Ceram Soc* 2012, **32**: 3369–3378.

[30] Sujith R, Srinivasan N, Kumar R. Small-scale deformation of pulsed electric current sintered silicon oxycarbide polymer derived ceramics. *Adv Eng Mater* 2013, DOI: 10.1002/adem.201300146.

[31] Konetschny C, Galusek D, Reschke S, *et al*. Dense silicon carbonitride ceramics by pyrolysis of cross-linked and warm pressed polysilazane powders. *J Eur Ceram Soc* 1999, **19**: 2789–2796.

[32] Weisbarth R, Jansen M. $SiBN_3C$ ceramic workpieces by pressureless pyrolysis without sintering aids: Preparation, characterization and electrical properties. *J Mater Chem* 2003, **13**: 2975–2978.